

Highly Impermeable “Soft” Self-Assembled Monolayers

Vijoleta Braach-Maksyutis* and Burkhard Raguse*

CSIRO Telecommunication & Industrial Physics
PO Box 218, Lindfield, NSW 2070, Australia

Received March 14, 2000

Revised Manuscript Received August 4, 2000

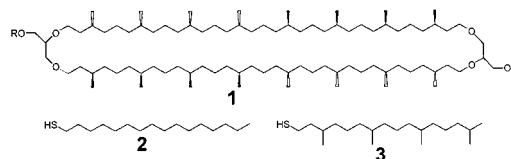
Self-assembled monolayers (SAMs) have been intensively investigated for a number of technological and scientific applications¹ such as corrosion resistant coatings,^{2,3} soft lithography,⁴ and molecular electronic devices.⁵ These applications require the ability to form thin films of well-defined and -controlled thickness, coupled with the formation of essentially insulating defect-free films.

However, fundamental problems exist for the formation of highly defect-free SAMs from commonly used, saturated alkanethiol molecules on substrates such as polycrystalline gold. Straight-chain alkanethiols with lengths greater than 12 carbons form crystalline monolayers. On Au substrates, the molecules align at an angle of 20–30° from normal to the surface.⁶ Formation of crystal domains, due to the tilt of the molecules, as well as due to steps and irregularities in the substrate lead to domain boundaries and crystal defects within the SAMs.⁷

An alternate approach to overcoming the sensitivity of the SAM to the substrate structure, that has not been previously explored, is to utilize the excellent barrier properties of archaeobacterial lipids. Archaeobacteria⁸ are extremophiles that thrive at elevated temperatures (>100 °C), at low pH, or in high salinity (1 M). A major structural feature which distinguishes these lipids from those of eukaryotes is the use of branched alkyl chains to retain the membrane in the critical liquid crystalline phase, rather than sacrificing chemical stability through the use of unsaturation.⁹ Chart 1 shows a typical archaeobacterial lipid (1) obtained from the *Sulfolobus* genus.⁸

The novel archae lipid mimic phytanylthiol 3 (PHT) was synthesized¹⁰ to study the effects of long-chain liquid crystalline phase lipids on the formation of self-assembled monolayers. The properties of PHT SAMs were compared to those of the crystalline hexadecanethiol 2 (HDT) SAMs. Hence, both molecules possess the same 16-carbon backbone but differ in their lipid phase properties.

Chart 1. Structures of Caldarcheol 1, a Typical Archaeobacterial Lipid Derived from *Sulfolobus* Genus,⁹ Hexadecanethiol 2, and the New Archae Lipid Mimic Phytanylthiol 3



The contact angle for HDT SAMs was comparable to those previously reported.¹¹ For example, the advancing contact angle for water was 110°. In comparison the water contact angle for the PHT SAMs was slightly lower at 106°. The contact angles for hexadecane solvent showed a similar trend. However, the advancing contact angle of hexadecane on the PHT SAM was only 37°, compared to 46° for the HDT SAM.

A lower contact angle has been previously observed for more disordered SAMs, such as short-chain alkanethiols or alkane thiols with bulky headgroups.¹¹ In the case of the longer phytanyl compounds the additional methyl groups projecting from the alkyl chain are known to prevent crystalline packing of the phytanyl chains,¹² with the resulting disorder leading to the observed decrease in contact angle.

Ellipsometry was used to further compare the PHT and HDT SAMs. The thickness of the HDT SAM was found to be 21.2 Å, whereas that of the PHT SAM was found to be 19.5 Å. As both HDT and PHT possess the same 16-carbon chain backbone it was expected that both molecules have similar lengths. This was confirmed using molecular modeling¹³ of the fully extended conformation. The calculated length (sulfur-to-terminal methyl group) for HDT was found to be 20.5 and 20.2 Å for PHT. Values for the ellipsometrically determined thickness of HDT SAMs from the literature^{6,11a,14} range from 19 to 25 Å, and FTIR indicated that the SAM-forming molecules assume an average tilt of 20–30° from the surface normal. The fact that the PHT SAM forms monolayers that have thickness similar to those of the HDT shows that the PHT forms close-packed SAMs similar to those of HDT SAMs.

The integrity and level of defects occurring in SAMs has been extensively studied using cyclic voltammetry (CV).^{6,15} We have used Fe(CN)₆³⁻ as a redox probe to establish a comparison between HDT and PHT SAMs. CV results using 1 mM Fe(CN)₆³⁻ in 1 M KCl are shown in Figure 1. As has been reported^{6,15} the HDT SAM prevents close approach of the Fe(CN)₆³⁻ to the Au electrode, forcing reduction to occur via tunneling across the SAM and/or at defect sites within the SAM.^{15b} SAMs formed from PHT showed a significantly smaller amount of Fe(CN)₆³⁻ reduction current (Figure 1). Since ellipsometry indicated a similar thickness for both the HDT and the PHT, either the PHT SAMs present an intrinsically higher barrier toward tunneling, or the PHT SAMs possess fewer defect than the HDT SAMs.

As a further test, an electrochemical corrosion method² was used to compare the barrier properties of PHT and HDT SAMs. This method relies on the electrochemical dissolution of Au at defects in the SAM structure in the presence of aqueous Br⁻. As

(1) Ulman, A. *An Introduction to Ultrathin Organic Films. From Langmuir–Blodgett to Self-Assembly*; Academic: San Diego, CA, 1991.

(2) Zamborini, F. P.; Crooks, R. M. *Langmuir* **1998**, *14*, 3279.

(3) French, M.; Creager, S. E. *Langmuir* **1998**, *14*, 2129.

(4) Kumar, A.; Whitesides, G. M. *Appl. Phys. Lett.* **1993**, *63*, 2002. Brittain, S.; Paul, K.; Zhao, X.-M.; Whitesides, G. M. *Physics World* **1998**, 31. Kumar, A.; Biebuyck, H. A.; Whitesides, G. M. *Langmuir* **1994**, *10*, 1498. Eberhardt, A. S.; Nyquist, R. M.; Parikh, A. N.; Zawodzinsky, T.; Swanson, B. I. *Langmuir* **1999**, *15*, 1595.

(5) Tour, J. M.; Kozaki, M.; Seminario, J. M. *J. Am. Chem. Soc.* **1998**, *120*, 8486. Cygan, M. T.; Dunbar, T. D.; Arnold, J. J.; Bumm, L. A.; Shedlock, N. F.; Burgin, T. P.; Jones, L., II; Allara, D. L.; Tour, J. M.; Weiss, P. S. *J. Am. Chem. Soc.* **1998**, *120*, 2721. Rampi, M. A.; Schueller, O. J. A.; Whitesides, G. M. *Appl. Phys. Lett.* **1998**, *72*, 1781. Haag, R.; Rampi, M. A.; Holmlin, R. E.; Whitesides, G. M. *J. Am. Chem. Soc.* **1999**, *121*, 7895.

(6) Porter, M. D.; Bright, T. B.; Allara, D. L.; Chidsey, C. E. D. *J. Am. Chem. Soc.* **1987**, *109*, 3559.

(7) Creager, S. E.; Hockett, L. A.; Rowe, G. K. *Langmuir* **1992**, *8*, 854. Chidsey, C. E. D.; Loiacono, D. N. *Langmuir* **1990**, *6*, 682. Finklea, H. O.; Hanshew, D. D. *J. Am. Chem. Soc.* **1992**, *114*, 3173.

(8) Kates, M.; Kushner, D. J.; Matheson, A. T., Eds. *The Biochemistry of Archae (Archaeobacteria)*; Elsevier Science Publishers: New York, 1993; p 261. De Rosa, M. *Thin Solid Films* **1996**, *284*, 13.

(9) Yamauchi, K.; Doi, K.; Kinoshita, M.; Kii, F.; Fukuda, H. *Biochim. Biophys. Acta* **1992**, *1110*, 171. Yamauchi, K.; Sakamoto, Y.; Moriya, A.; Yamada, K.; Hosokawa, T.; Higuchi, T.; Kinoshita, M. *J. Am. Chem. Soc.* **1990**, *112*, 3188. Yamauchi, K.; Doi, K.; Yoshida, Y.; Kinoshita, M. *Biochim. Biophys. Acta* **1992**, *1146*, 178.

(10) PHT was synthesised by treatment of phytanyl bromide with thiourea followed by alkaline hydrolysis. See Supporting Information for full experimental details.

(11) (a) Bain, C. D.; Troughton, E. B.; Tao, Y.-T.; Evall, J.; Whitesides, G. M.; Nuzzo, R. G. *J. Am. Chem. Soc.* **1989**, *111*, 321. (b) Laibinis, P. E.; Whitesides, G. M.; Allara, D. L.; Tao, Y.-T.; Parikh, A. N.; Nuzzo, R. G. *J. Am. Chem. Soc.* **1991**, *113*, 7152.

(12) Lindsey, H.; Petersen, N. O.; Chan, S. I. *Biochim. Biophys. Acta* **1979**, *555*, 147.

(13) Chem3D; CambridgeSoft Corporation: Cambridge, MA, 1999.

(14) Biebuyck, H. A.; Bain, C. D.; Whitesides, G. M. *Langmuir* **1994**, *10*, 1825.

(15) (a) Miller, C. J.; Cuendet, P.; Graetzel, M. *J. Phys. Chem.* **1991**, *95*, 877. (b) Becka, A. M.; Miller, C. J. *J. Phys. Chem.* **1992**, *96*, 2657.

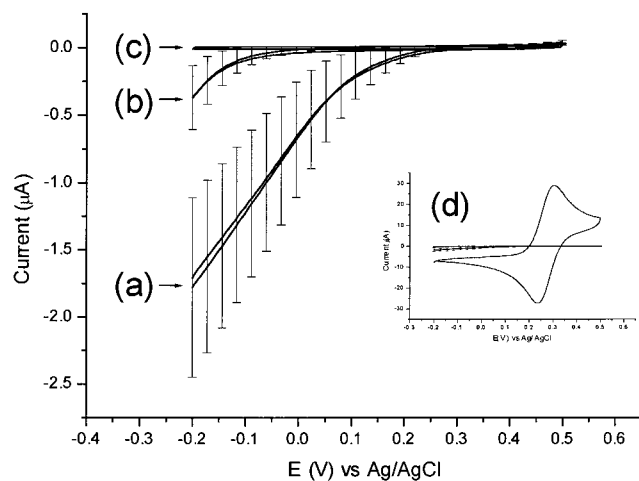


Figure 1. Cyclic voltammogram scans obtained in aqueous electrolyte solution containing 1 mM $\text{K}_3\text{Fe}(\text{CN})_6$ in 1 M KCl. (a) Au electrode coated with HDT and (b) Au electrode coated with PHT. (c) Au electrode coated with PHT or HDT in the absence of the $\text{K}_3\text{Fe}(\text{CN})_6$ redox probe. The inset (d) shows the $\text{K}_3\text{Fe}(\text{CN})_6$ cyclic voltammogram of a bare gold electrode superimposed onto the response for electrodes (a) to (c). Sweep rate was 100 mV/s. Reference electrode was Ag/AgCl. The working electrode area was 14 mm². Results are the average of 20 separate electrode measurements. The 1st and 20th sweep were essentially superimposable. Error bars indicate ± 1 standard deviation.

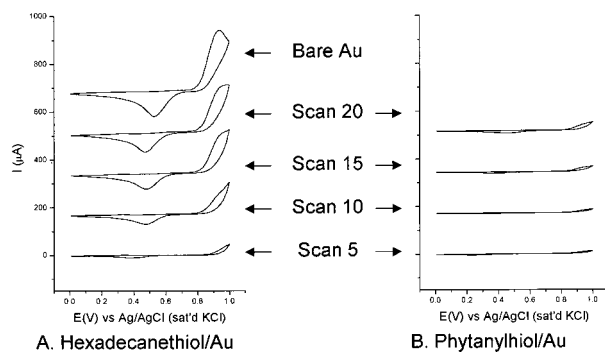


Figure 2. Repeated cyclic voltammogram scans obtained in aqueous electrolyte solution containing 0.1 M $\text{HClO}_4/0.01$ M KBr from 0 to 1 V vs Ag/AgCl at 50 mV/s of (a) Au electrode coated with HDT and (b) Au electrode coated with PHT. The electrode area was 14 mm². For clarity only every fifth scan is shown.

the Br^- ion is significantly smaller than the $\text{Fe}(\text{CN})_6^{3-}$ ion it may be expected that this test is more sensitive toward smaller defects. The thin hydrocarbon barrier formed by a SAM prevents the Br^- from attacking the Au surface. However, at defect sites in the SAM film the Br^- is able to dissolve the Au. Each CV sweep the size of the corroded area increases, and thus the current passing through the electrode increases. Fewer defects in the SAM structure should lead to a slower increase in Au dissolution.

Figure 2 shows CVs of bare Au and of the HDT- and PHT-modified Au surfaces. For clarity, every fifth CV scan up to 20 scans is shown. Figure 2 shows the maximum anodic current against the CV scan number. The anodic peak starting at 0.8–0.9 V is interpreted as being due to Au dissolution in the presence of Br^- , while the cathodic peak at 0.5 V corresponds to the redeposition of Au.²

The CV for the HDT SAMs (Figure 2a) displayed similar behavior to those reported by Zamborini and Crooks.² The HDT SAM protects the Au electrode surface, resulting in a relatively small current passing through the electrode. After 20 scans, however, the CV resembled that of a bare Au electrode (Figure 2a), indicating removal of the HDT SAM. The initial CV scan showed relatively high anodic currents at 1 V that decreased after the initial scan (Figure 3).²

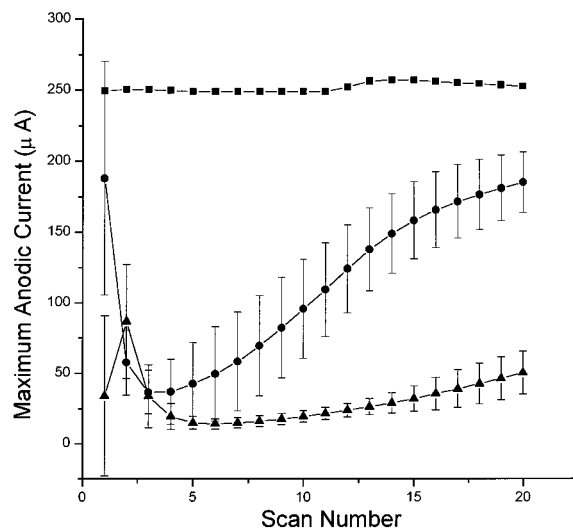


Figure 3. Maximum anodic current against the number of CV scans. Scans were taken from 0 to 1 V vs Ag/AgCl in 0.1 M $\text{HClO}_4/0.01$ M KBr electrolyte solution at a scan rate of 50 mV/s. The electrode area was 14 mm². (a) bare Au electrode -■- (b) HDT-coated Au electrode -●- (c) PHT-coated Au electrode -▲-. Error bars indicate ± 1 standard deviation. Lines are provided as a guide to the eye.

In contrast the CVs of PHT SAM-coated Au electrodes (Figure 2b) were significantly different. First, the anodic current was lower than that obtained for the HDT SAMs, and second, the rate of increase of the anodic current at 1 V is lower for the PHT SAM compared to that of the HDT SAM (Figure 3). For instance, after 20 scans the maximum anodic current for HDT SAMs has changed from a minimum of 36 ± 15 to 185 ± 21 μA , whereas the maximum anodic current of the PHT SAMs began with a minimum of 14 ± 44 reaching 50 ± 15 μA .

The PHT SAM therefore provides significantly better barrier properties compared to the SAM formed from the crystalline HDT SAM, even though both molecules are hydrophobic and form SAM structures of essentially the same thickness. Zamborini and Crooks² postulated that the reason that the HDT SAMs undergo relatively rapid pitting corrosion is due to the crystallinity of the SAMs. We believe that the enhanced passivating properties of the PHT SAMs may arise from the dynamic property of liquid crystallinity which may impart a “self-healing” effect on SAM defects. Previous reports on the failure of disordered molecules to form defect-free SAMs on metals used short-chain alkanethiols. The key to the defects may have been the short length of these molecules rather than their liquid crystalline phase property. The longer length PHT SAM does not exhibit the same defect properties which were observed for the short alkanethiols.¹¹

Self-assembled monolayers were formed from a new class of SAM-forming molecules based on archae lipid features. Contact angle measurements indicated that the PHT SAM is more disordered than the HDT SAMs. The ellipsometric thickness of the PHT SAMs is comparable to that of HDT SAMs. Finally, CV measurements using both the redox and electrochemical corrosion techniques indicated that PHT SAMs may have fewer defects than HDT SAMs. We have shown that coupling a dynamic disordering property to a longer length molecule such as PHT, creates a superior barrier performance compared to crystalline HDT SAMs of similar thickness.

Acknowledgment. We thank Mr. L. Wieszorek for assistance in obtaining the ellipsometry data.

Supporting Information Available: Supporting Information: synthesis of PHT 3, preparation of the SAM coated Au electrodes, CV measurements, contact angles (PDF). This material is available free of charge via the Internet at <http://pubs.acs.org>.